

UCSF

UC San Francisco Previously Published Works

Title

Loss of Foveal Cone Structure Precedes Loss of Visual Acuity in Patients With Rod-Cone Degeneration

Permalink

<https://escholarship.org/uc/item/3s9946z8>

Journal

Investigative Ophthalmology & Visual Science, 60(8)

ISSN

0146-0404

Authors

Bensinger, Ethan

Rinella, Nicholas

Saud, Asma

et al.

Publication Date

2019-07-23

DOI

10.1167/iovs.18-26245

Copyright Information

This work is made available under the terms of a Creative Commons Attribution-NonCommercial-NoDerivatives License, available at

<https://creativecommons.org/licenses/by-nc-nd/4.0/>

Peer reviewed

Loss of Foveal Cone Structure Precedes Loss of Visual Acuity in Patients With Rod-Cone Degeneration

Ethan Bensinger,¹ Nicholas Rinella,² Asma Saud,² Panagiota Loumou,² Kavitha Ratnam,¹ Shane Griffin,² Jia Qin,² Travis C. Porco,^{2,3} Austin Roorda,¹ and Jacque L. Duncan²

¹School of Optometry and Vision Science Graduate Group, University of California, Berkeley, California, United States

²Department of Ophthalmology, University of California, San Francisco, California, United States

³Proctor Foundation, Department of Ophthalmology, University of California, San Francisco, California, United States

Correspondence: Jacque L. Duncan, 10 Koret Way, K113, San Francisco, CA 94143-0730, USA; Jacque.duncan@ucsf.edu.

Submitted: November 20, 2018

Accepted: June 13, 2019

Citation: Bensinger E, Rinella N, Saud A, et al. Loss of foveal cone structure precedes loss of visual acuity in patients with rod-cone degeneration. *Invest Ophthalmol Vis Sci*. 2019;60:3187–3196. <https://doi.org/10.1167/iov.18-26245>

PURPOSE. To assess the relationship between cone spacing and visual acuity in eyes with rod-cone degeneration (RCD) followed longitudinally.

METHODS. High-resolution images of the retina were obtained using adaptive optics scanning laser ophthalmoscopy from 13 eyes of nine RCD patients and 13 eyes of eight healthy subjects at two sessions separated by 10 or more months (mean 765 days, range 311–1935 days). Cone spacing Z-score measured as close as possible (average $<0.25^\circ$) to the preferred retinal locus was compared with visual acuity (letters read on the Early Treatment of Diabetic Retinopathy Study [ETDRS] chart and logMAR) and foveal sensitivity.

RESULTS. Cone spacing was significantly correlated with ETDRS letters read ($\rho = -0.47$, 95%CI -0.67 to -0.24), logMAR ($\rho = 0.46$, 95%CI 0.24 to 0.66), and foveal sensitivity ($\rho = -0.30$, 95%CI -0.52 to -0.018). There was a small but significant increase in mean cone spacing Z-score during follow-up of $+0.97$ (95%CI 0.57 to 1.4) in RCD patients, but not in healthy eyes, and there was no significant change in any measure of visual acuity.

CONCLUSIONS. Cone spacing was correlated with visual acuity and foveal sensitivity. In RCD patients, cone spacing increased during follow-up, while visual acuity did not change significantly. Cone spacing Z-score may be a more sensitive measure of cone loss at the fovea than visual acuity in patients with RCD.

Keywords: adaptive optics scanning laser ophthalmoscopy, retinal degeneration, cones

Rod-cone degeneration (RCD) causes progressive death of photoreceptors with consequent vision loss over many years.¹ The slowly progressive nature of RCD makes it challenging to reliably monitor changes during a period of 1 or 2 years. In RCD, night vision and peripheral vision are lost earliest, but visual acuity can remain stable and normal until advanced stages of disease.¹ A longitudinal study of patients with retinitis pigmentosa (RP) followed for 9 years found that visual acuity had the slowest decline relative to other measures, such as visual field area and focal electroretinogram (ERG).² In addition, foveal measures of visual function demonstrate increased variability as retinal degeneration progresses.³ Robust, sensitive measures of foveal health and cone loss, particularly ones that rely on structural measures rather than subjective psychophysical measures described above, could facilitate measurement of disease progression in patients with RCD.

Objective measures of retinal structure have become widely used because of advances in noninvasive, high-resolution imaging modalities that can be used to monitor changes in retinal and foveal topography. Spectral-domain optical coherence tomography (SD-OCT), for example, provides noninvasive, cross-sectional measures of retinal structures, including photoreceptors.^{4,5} SD-OCT measures of outer retinal thickness have been shown to correlate with visual field sensitivity in eyes with RP,^{6,7} and may provide a useful, objective outcome measure for clinical trials.^{4,8} Adaptive-optics scanning laser

ophthalmoscopy (AOSLO) allows for en face visualization of cone mosaics and measurements of cone spacing and density in healthy and diseased eyes.^{9–11} Modern AOSLO systems are capable of imaging the cone mosaic at the fovea and yield measures of cone spacing^{12–18} that are comparable to histologic studies.¹⁹

Objective, structural measures of cone spacing may be more reliable than functional measures, but they are meaningful for patients only if visual function correlates with retinal structure. In cross-sectional studies of RCD patients, increases in cone spacing at or near the fovea were shown to correlate with visual acuity declines in a nonlinear way.^{17,18} Visual acuity decreased below 20/25 only in patients whose foveal cone density was 40% to 60% lower than normal, suggesting that visual acuity is preserved despite significant cone loss and is not a sensitive measure of foveal cone integrity.^{17,18} One limitation of prior cross-sectional studies, however, was that we could not know the extent to which the low cone densities resulted from actual cone loss or simply reflected the lower end of the spectrum of normal variation in cone density.

To understand how acuity changes during degeneration it would be desirable to track photoreceptor structure and function over time in the same RCD patients. Intervisit and interobserver variability in cone spacing measures from AOSLO images have been quantified in healthy eyes and eyes with RCD; cone changes measured over time that are greater than baseline intervisit and interobserver variability are likely to represent

disease progression in RCD patients.²⁰ In this retrospective study, we compared foveal cone spacing with best-corrected visual acuity (BCVA) in patients with RCD and healthy subjects monitored longitudinally during periods ranging from 10 months to 5 years to characterize changes in foveal structure and function during disease progression in eyes with RCD.

METHODS

Study Design

Procedures for this study were followed in accordance with the Declaration of Helsinki, and informed consent was given by all subjects. The study protocol was approved by the institutional review boards of the University of California, San Francisco and the University of California, Berkeley.

Subjects

This retrospective study included healthy adults and patients with RCD, all with visual acuity of 20/40 or better in whom cone mosaics were visualized in the foveal region using AOSLO during two sessions separated by at least 10 months. The subjects are described in the Table.

Functional Measurements

Visual acuity was measured as the number of letters read correctly using standard eye charts, according to the Early Treatment of Diabetic Retinopathy Study (ETDRS) protocol²¹; results were also converted to the logMAR. Foveal sensitivity was measured in decibels from automated static perimetry measuring macular sensitivity in the central 20° (Humphrey visual field 10-2 protocol; Carl Zeiss Meditech, Dublin, CA, USA).

SD-OCT Imaging and Analysis

SD-OCT images (Spectralis HRA+OCT; Heidelberg Engineering, Vista, CA, USA) were acquired through the foveal center by asking the patient to look at a central fixation target, such that the foveal center on OCT scans included the preferred retinal locus for fixation (PRL). Automated retinal tracking was used to average 100 B-scans in 20° horizontal and vertical cross sections through the PRL. Horizontal SD-OCT scans through the PRL were exported to data analysis software (Igor Pro; WaveMetrics, Inc., Portland, OR, USA) and manually segmented using subroutines^{5,6,22-24} to identify boundaries between the different retinal layers. The specific measurement made for the purposes of this study was the thickness of the cone outer segment plus RPE (referred to as OS+²²) at the PRL defined from AOSLO images as described below.

AOSLO Imaging and Cone Spacing Measurements

Prior to AOSLO imaging, pupils were dilated with 1% tropicamide and 2.5% phenylephrine. High-resolution images of the fovea were acquired using a confocal AOSLO system¹² and processed into montages as described previously.⁹ The PRL for fixation was localized in the AOSLO images by presenting a target through modulation of the AOSLO scanning raster and 10-second videos were recorded while the patient fixated on the target.¹⁸ The PRL was computed as the centroid of the scatter plot of the fixated target positions on the retina. AOSLO images that demonstrated clear cone mosaics at or near the PRL were compared with precisely aligned and superimposed SD-OCT scans through the PRL to confirm the cone profiles corresponded to cross-sectional images with visible external

limiting membrane and inner segment/outer segment or ellipsoid zone bands, and then were selected for cone spacing. Customized software was used to determine cone spacing using previously described methods.⁹ Other metrics for analyzing cones in AOSLO images that are potentially more sensitive than cone spacing were considered²⁵; however, limited resolution of the AOSLO images acquired near the fovea in this study necessitated the robustness provided by cone spacing. In order to most accurately study the cones involved in fine visual acuity, cone spacing at baseline and subsequent visits at least 10 months later was measured within the region of highest cone resolution and closest to the PRL at each visit. Due to changes in image quality over time, the region of highest cone resolution that permitted reliable cone identification was not always the same at the baseline and follow-up visits. The highest resolution cone spacing location for each visit was measured as an eccentricity in degrees relative to the PRL, because we were unable to identify the exact location of the anatomic fovea (point of maximum cone density). However, this is a small error because the PRL location relative to the point of maximum cone density is reported in the literature to average approximately 35 μm or 7 arcmin.^{16,26-28} In this manuscript, we assume that offsets between the PRL and the point of maximum cone density are no different between RCD patients and normal. To account for changes between visits in cone spacing with respect to eccentricity relative to the PRL,¹⁹ cone spacing values were converted to Z-scores, or the number of standard deviations (SD) from the normal mean (based on 37 age-similar healthy eyes ranging in age from 14–79 years, mean 36.9 years),¹⁸ at the eccentricity from the PRL where cones were measured. Our decision to do this rested on an assumption that Z-scores and changes in Z-scores at the measured location should reflect similar changes at the PRL. Previous observations of diffuse changes in cone density throughout the central region in RCD patients^{9,11,17,29,30} support this assumption. Z-scores between -2 and +2 SD were considered normal; Z-scores greater than 2 indicated increased cone spacing due to cone loss. All measures were acquired at baseline and at least 10 months later in each eye studied.

Statistical Analysis

Structural measures (cone-spacing Z-scores and OCT measurement of OS+ thickness at the PRL) were compared with each other using Spearman's rank correlation ρ , with 95% confidence intervals that do not contain zero considered statically significant. Structural measures (cone spacing Z-score and OS+ thickness) were compared with functional measures, including ETDRS letters read, logMAR, and foveal sensitivity, at each time point using Spearman's rank correlation ρ with 95% confidence intervals, clustered by individual to account for the fact that each individual was measured at baseline and follow-up. The Wilcoxon signed rank test was used to analyze change in measures over time for each subject with $P < 0.05$ considered statistically significant.

RESULTS

Clinical Characteristics

Clinical characteristics of the subjects are shown in the Table. Thirteen eyes from nine patients with RCD were studied. Of 13 eyes, 11 had RP, one had Usher syndrome type 2C, and one had Usher syndrome type 3A. Thirteen eyes of eight healthy subjects were also studied. The nine patients ranged in age from 28 to 42 years at baseline (mean 35), and the eight

TABLE. Summary of Clinical Characteristics

ID	Eye	Patient Information				Function				Structure			
		Axial Length, mm	Age/ Sex, Bl, Fu	Follow-up Duration, mo	Diagnosis	Visual Acuity, Bl, Fu	ETDRS Letters, Bl, Fu	logMAR, Bl, Fu	Foveal Sensitivity (dB), Bl, Fu	Cone Spacing Z-Score, Bl, Fu	Average Eccentricity From PRL (degrees), Bl, Fu	OS+ Thickness at PRL (µm), Bl, Fu	
													Function
10046	OS	22.04	28, 33/F	63	ADRP: NR2E3 p.Gly56 Arg/+	20/25, 20/20	82, 85	0.1, 0	39, 37	2.35, 2.98	0.048, 0.051	71.3, 78.4	
40073	OD	24.53	32, 35/F	35	ADRP <i>PRPF31</i>	20/16, 20/16	93, 91	-0.1, -0.1	37, 40	1.06, 3.71	0.068, 0.49	77.9, 72.5	
	OS	24.78		35	c.239delG, p.?:+ (deletion of G at position -1 in IVS3, affects mRNA splicing)	20/13, 20/16	94, 89	-0.2, -0.1	37, 40	0.88, 1.61	0.074, 0.49	78.2, 75.8	
30019	OD	22.69	37, 39/F	21	ADRP: <i>RHO</i>	20/16, 20/25	89, 79	-0.1, 0.1	37, 36	1.52, 3.14	0.35, 0.046	67.1, 58.6	
40041	OD	26.58	39, 40/F	13	p.Gly51Val/+	20/20, 20/20	84, 85	0, 0	39, 39	0.85, 2.13	0.12, 0.34	71.2, 72.8	
	OS	26.17		13	<i>USH2A</i> p. Cys759Phe/c.8682-3T>G splice site mutation	20/25, 20/25	80, 81	0.1, 0.1	40, 39	1.08, 0.82	0.034, 0.048	72.4, 79.2	
30015	OD	23.96	39, 40/M	13	Simplex RP	20/20, 20/20	83, 84	0, 0	37, 37	1.56, 2.23	0.21, 0.056	74.4, 70.3	
40026	OD	22.83	28, 29/F	12	Simplex RP	20/25, 20/20	83, 84	0.1, 0	32, 33	3.11, 5.23	0.23, 0.098	77.7, 79.8	
	OS	22.72				20/20, 20/25	84, 80	0, 0.1	32, 32	2.39, 4.17	0.072, 0.51	78.3, 75.4	
40039	OD	23.35	42, 45/F	36	ARRP	20/20, 20/16	90, 91	0, -0.1	36, 38	1.97, 2.39	0.073, 0.12	78.3, 71.7	
	OS	23.24		36	<i>USH2A</i> p. Cys759Phe/ p.Cys766Arg	20/16, 20/16	91, 89	-0.1, -0.1	39, 38	1.77, 0.63	0.053, 0.34	71.2, 78.2	
30013	OD	23.20	33, 34/M	12	<i>USH2C: GPR98</i>	20/20, 20/16	85, 92	0, -0.1	36, 27	2.12, 2.93	0.045, 0.055	70.1, 64.1	
					p.Thr2875, Lysis*2/, p.Met5890, Valis*10								
30007	OD	22.44	33, 36/F	43	<i>USH3A: clarin-1</i>	20/32, 20/20	74, 85	0.2, 0	38, 35	-0.30, 1.01	0.66, 0.20	78.2, 82.7	
					p.Asn48Lys/								
					p.Asn48Lys								
10023	OD	23.46	57, 58/M	12	Normal	20/10, 20/13	99, 95	-0.30, -0.19	37, 38	0.98, -0.021	0.034, 0.45	77.4, 69.3	
	OS	23.27		12		20/13, 20/10	98, 100	-0.19, -0.30	37, 35	1.50, 0.89	0.16, 0.17	77.5, 77.6	
10033	OD	23.91	57, 58 M	10	Normal	20/16, 20/16	93, 90	-0.1, -0.1	--, 34	1.70, 1.28	0.045, 0.047	64.5, 64.3	
	OS	24.03		12		20/16, 20/20	93, 85	-0.1, 0	--, 36	1.00, 1.27	0.051, 0.061	72.1, 67.1	
40051	OD	23.74	48, 49/M	12	Normal	20/13, 20/16	95, 93	-0.19, -0.1	39, 37	0.01, 1.22	0.32, 0.054	76.5, 84.2	
	OS	23.68		12		20/13, 20/16	95, 93	-0.19, -0.1	43, 36	1.54, 1.21	0.039, 0.069	71.7, 72.3	
40053	OD	23.74	37, 40/F	37	Normal	20/20, 20/16	84, 89	0, -0.1	37, 40	0.85, 0.33	0.27, 0.47	75.0, 79.7	
	OS	24.00		37		20/13, 20/16	95, 91	-0.19, -0.1	39, 37	1.15, -0.21	0.20, 0.4	79.8, 78.6	
40055	OD	23.96	50, 53/M	35	Normal	20/13, 20/13	98, 97	-0.19, -0.19	37, 38	-0.14, -0.05	0.41, 0.56	91.8, 86.3	
	OS	23.87	50, 51	12		20/16, 20/16	90, 93	-0.1, -0.1	39, 39	0.21, -0.20	0.22, 0.45	89.3, 83.8	
40054	OS	25.31	24, 27	36	Normal	20/16, 20/16	92, 90	-0.1, -0.1	39, 37	0.16, 0.04	0.47, 0.56	84.2, 86.7	
40061	OS	24.14	50, 53	36	Normal	20/16, 20/13	93, 95	-0.1, -0.19	38, 37	-0.57, 0.68	0.47, 0.59	77.7, 84.5	
40048	OD	23.73	51, 53	24	Normal	20/13, 20/13	95, 95	-0.19, -0.19	38, 36	-0.59, 0.30	0.53, 0.53	86.5, 79.5	

Bl, baseline; Fu, follow-up; AD, autosomal dominant; AR, autosomal recessive; *USH2C*, Usher syndrome type 2C; *USH3A*, Usher syndrome type 3A. Foveal sensitivity was not measured at baseline in 10033. Both eyes of 40055 were imaged at baseline and 12 months, but the right eye was imaged again at 36 months. For each subject, age is listed in years, and the time between imaging dates 1 and 2 is shown in months.

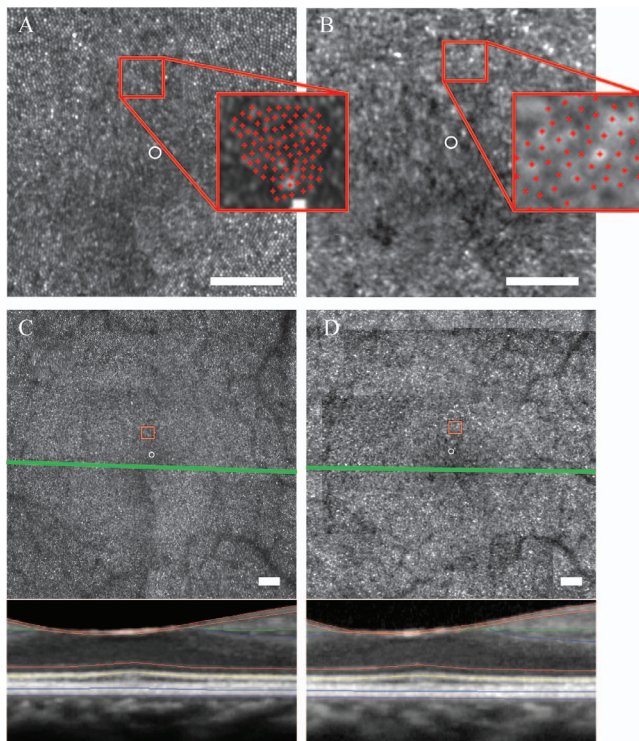


FIGURE 1. AOSLO Images of foveal mosaic for RCD patient 40073 at two time points separated by 36 months, with baseline image to the top left (A) and follow-up image to the top right (B). AOSLO images over a larger area are shown at baseline at the bottom left (C) and at follow-up at the bottom right (D) with the green line depicting the location of the SD-OCT B-scan and segmented SD-OCT B-scan shown below. The scale bar is 0.25° and the scales are the same between the two images. The PRL is indicated by the white circle. Insets to the right of each image show the cone locations used to compute cone spacing (red crosses).

healthy subjects ranged from 24 to 57 years at baseline (mean 47); the healthy subjects were significantly older than the patients (Wilcoxon rank sum test with continuity correction test $P = 0.015$). AOSLO images were taken at two time points separated by greater than 10 months (mean 765 days, range 311–1935 days) for each of the eyes. There was no significant difference in duration of follow-up between patients and controls (mean follow up in patients = 845.9 days, mean follow-up in healthy subjects = 736.8 days, Wilcoxon test $P = 0.49$).

Structural Measures

The PRL was used as the origin to compute the eccentricity of locations where cones were measured and was recorded at each visit. There was slight variation between baseline and follow-up in the precise location of the PRL for each AOSLO image (mean difference = 0.128° , SD = 0.078; average change in patients = 0.120° , SD = 0.088; average change in control subjects = 0.135° , SD = 0.061), which has a minimal effect on the cone spacing Z-score (mean absolute Z-score change due to PRL change = 0.151, range 0.0354–0.368). We attribute the slight change in PRL between visits to a combination of some variability due to the limited 10-second video duration used to assess the PRL and slight image registration errors. Figure 1 shows examples of foveal cone images near the PRL, the OCT B-scan location and segmentation image, and identification of cones for cone spacing measures in patient 40073; a white circle indicates the center of mass of the displayed fixational

eye positions at the PRL. Additional foveal cone images near the PRL for patient 40026 and healthy subject 40051 are shown in Supplementary Figure S1. Figure 2 plots cone spacing Z-scores against the distances from the PRL where measures were made in healthy subjects and patients. The average eccentricities of the cone spacing measures were slightly greater at the second visit than the first visit for both healthy subjects and RCD patients (mean baseline eccentricity = 0.21° , mean follow-up eccentricity = 0.27° ; mean difference for normal subjects = 0.06° , 95%CI -0.14 to 0.0010 ; mean difference for patients = 0.07° , 95%CI -0.19 to 0.054). Note that the Z-scores are greater than 0 for most measurements made closest to the fovea. This is not unexpected in the RCD patients, but in the healthy eyes we might expect the Z-scores to average around 0. The increase in Z-scores here reflects our bias toward selecting healthy eyes with clear and unambiguous cones near the fovea, which in turn are the eyes in which spacing falls in the upper range of the normal distribution. It should be noted that despite the bias, the Z-scores in healthy eyes are all lower than 2 and therefore fall within the normal range (Fig. 2). Furthermore, the study focuses on the changes over time, and we have no reason to believe that this selection bias will influence that analysis in any way.

There was a small but significant increase in cone spacing Z-score during follow up in the RCD patients of $+0.97$ (95%CI 0.57 – 1.4), while there was no significant change in Z-score in healthy eyes (-0.070 , 95%CI -0.41 to 0.27 ; Fig. 3, top). Some patients with the longest follow-up showed little change, while others with shorter follow-up showed greater change, indicating variability in the rate of progression. Changes in cone spacing Z-score for each eye are shown in Supplementary Figure S2.

Mean SD-OCT OS+ thickness at the PRL was not significantly thinner in RCD patients than healthy subjects at baseline or at follow-up (mean difference between healthy and patients at baseline = $4.2 \mu\text{m}$, 97.5% CI -0.28 to $8.8 \mu\text{m}$; at follow-up = $4.2 \mu\text{m}$, 97.5%CI -1.4 to $9.7 \mu\text{m}$). SD-OCT OS+ thickness at the PRL did not change significantly during follow-up in healthy eyes ($+0.70 \mu\text{m}$, 95%CI -1.5 to $3.0 \mu\text{m}$, or patients with RCD [$+0.64 \mu\text{m}$, -1.9 to $3.2 \mu\text{m}$]; Fig. 3, bottom). SD-OCT OS+ thickness at the PRL was negatively correlated with cone spacing Z-score in healthy eyes at baseline ($\rho = -0.55$, 95%CI -0.86 to -0.031) and at the follow-up exam ($\rho = -0.64$, 95%CI -0.93 to -0.17). However, in RCD patients OS+ thickness was not correlated with Z-score at baseline ($\rho = -0.019$, 95%CI -0.55 to 0.47), or follow-up ($\rho = -0.011$, 95%CI -0.64 to 0.52 ; Fig. 4). When all subjects at all dates were aggregated together there was a significant correlation between OS+ thickness and Z-score ($\rho = -0.40$, 95%CI -0.67 to -0.087).

Functional Measures

There was no significant change in visual acuity measured as ETDRS letters read or logMAR or in foveal sensitivity between imaging sessions in the healthy subjects. Despite a significant increase in cone spacing Z-score during follow-up in the RCD patients of $+0.97$ (see above) there was no significant change in letters read (average change -0.71 letters, 95%CI -2.1 to 0.78), logMAR (average change -0.0074 , 95%CI -0.043 to 0.024) or foveal sensitivity (average change -0.36 dB, 95%CI -1.56 to 0.88).

Structure Versus Function

When all study subjects and visits were combined, cone spacing Z-score was significantly correlated with ETDRS letters read ($\rho = -0.47$, 95%CI -0.67 to -0.24), logMAR ($\rho = 0.46$, 95%CI 0.26 to 0.66) and foveal sensitivity ($\rho = -0.30$,

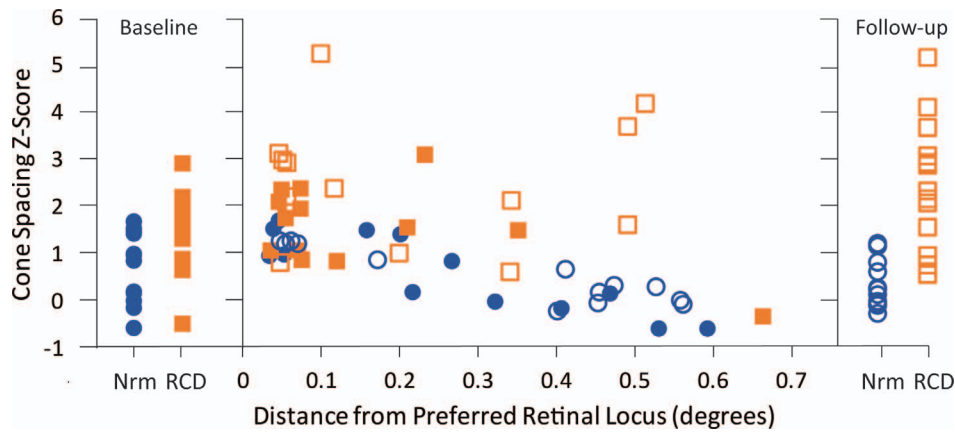


FIGURE 2. Cone spacing Z-score for all baseline measures shown on the *left* for normal (Nrm) and RCD patients. Cone spacing Z-score plotted against the distance from the measurement to the AOSLO derived PRL shown in the *center*. Cone spacing Z-score for all follow-up measures shown on the *right*. Cone spacing measures taken at baseline are shown as *filled symbols* and follow-up measures are shown as *open symbols*; RCD patients are shown as *orange squares*, healthy subjects are shown as *blue circles*.

95%CI -0.52 to -0.018 ; Fig. 5). LogMAR is not shown because it is derived from ETDRS letters read. OS+ thickness was not significantly correlated with ETDRS letters read ($\rho = -0.11$, 95%CI -0.46 to 0.19) or foveal sensitivity when all subjects and visits were combined ($\rho = 0.026$, 95%CI -0.26 to 0.28 ; Fig. 6).

Analyzing subgroups and times separately, cone spacing Z-score was significantly correlated with foveal sensitivity at baseline ($\rho = -0.55$, 95%CI -0.94 to -0.05) but not follow-up ($\rho = -0.42$, 95%CI -0.77 to 0.084) in RCD patients. In healthy subjects, at baseline there was no significant correlation between Z-score and foveal sensitivity ($\rho = 0.15$, 95%CI

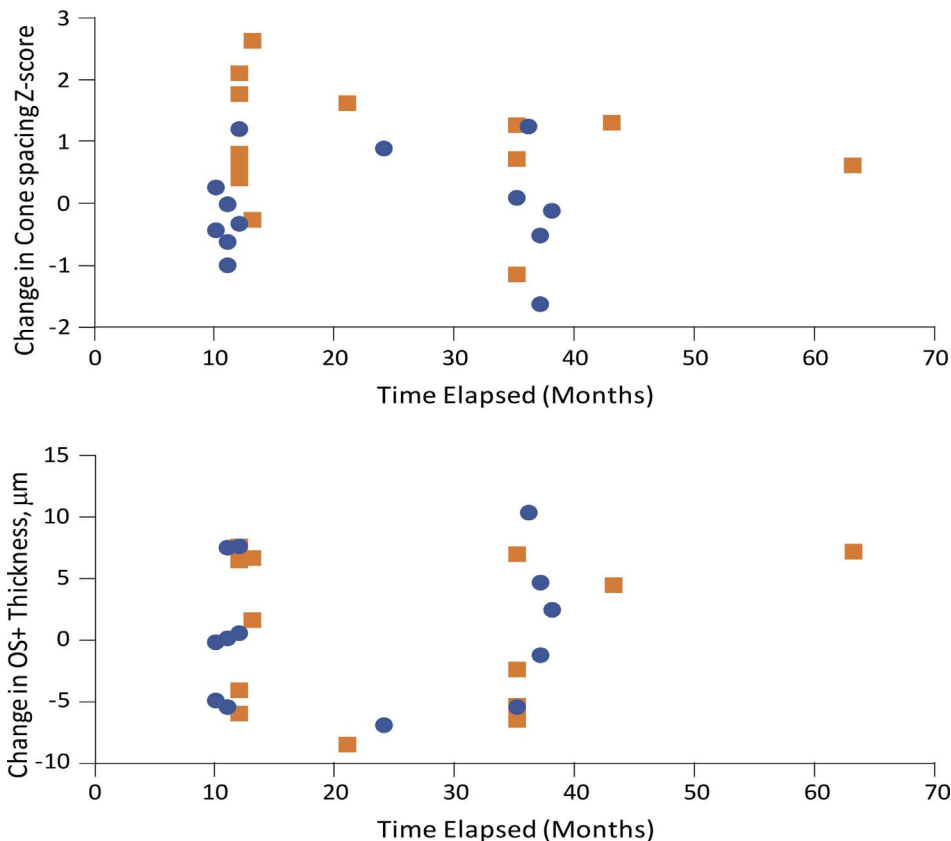


FIGURE 3. Change in cone spacing Z-score (*top*) and change in OS+ thickness (*bottom*) plotted against the time in months between the first imaging date and second imaging date. RCD patients are shown with *orange squares*, normal with *blue circles*. There was a small, significant increase in Z-score in RCD patients (average change = $+0.97$ [95%CI 0.57 to 1.4], while no significant changes were found in healthy subjects (average change = -0.070 , 95%CI -0.42 to 0.27). There was no significant change in OS+ thickness in patients with RCD ($+0.64 \mu\text{m}$, 95%CI -1.9 to $3.2 \mu\text{m}$) or healthy subjects ($+0.70 \mu\text{m}$, 95%CI -1.5 to $3.0 \mu\text{m}$).

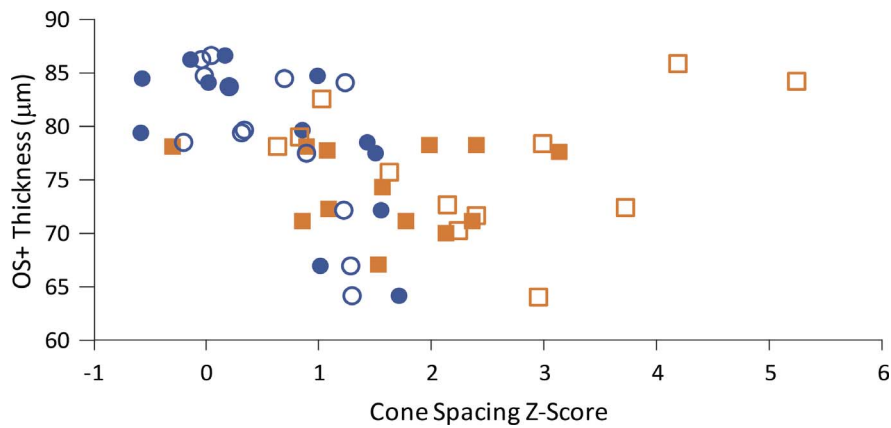


FIGURE 4. OS+ thickness compared with cone spacing Z-score. Measures taken on first imaging date shown as *filled symbols* and follow-up shown as *open symbols*; RCD patients are shown as *orange squares*, healthy subjects are shown as *blue circles*. SD-OCT OS+ thickness at the PRL was negatively correlated with cone spacing Z-score in healthy eyes at baseline ($\rho = -0.55$, 95%CI -0.86 to -0.048) and at the follow-up exam ($\rho = -0.64$, 95%CI -0.93 to -0.17). However, in RCD patients OS+ thickness was not correlated with Z-score at baseline ($\rho = -0.019$, 95%CI -0.55 to 0.47) or follow-up ($\rho = -0.011$, 95%CI -0.64 to 0.52). When all subjects at all dates were aggregated together there was a significant correlation between OS+ thickness and Z-score ($\rho = -0.40$, 95%CI -0.67 to -0.087).

-0.57 to 0.79), but there was a significant correlation at follow-up ($\rho = -0.62$, 95%CI -0.83 to -0.26).

DISCUSSION

This retrospective study is the first to assess longitudinal changes in foveal cone spacing in patients with RCD and healthy eyes followed for at least 10 months, and to relate changes in cone spacing to clinical measures of foveal function

and outer retinal thickness. The results represent an important continuation of a prior cross-sectional study in RCD patients that identified a significant, nonlinear correlation between foveal cone spacing and function.¹⁸ Over the course of the longitudinal study, there was no measurable change in visual function (VA and foveal sensitivity), yet a small but significant amount of cone loss was detected. The increase in cone spacing in RCD patients is consistent with prior reports.¹¹ We also confirmed that cone spacing Z-score was correlated with measures of visual function at the fovea.¹⁸

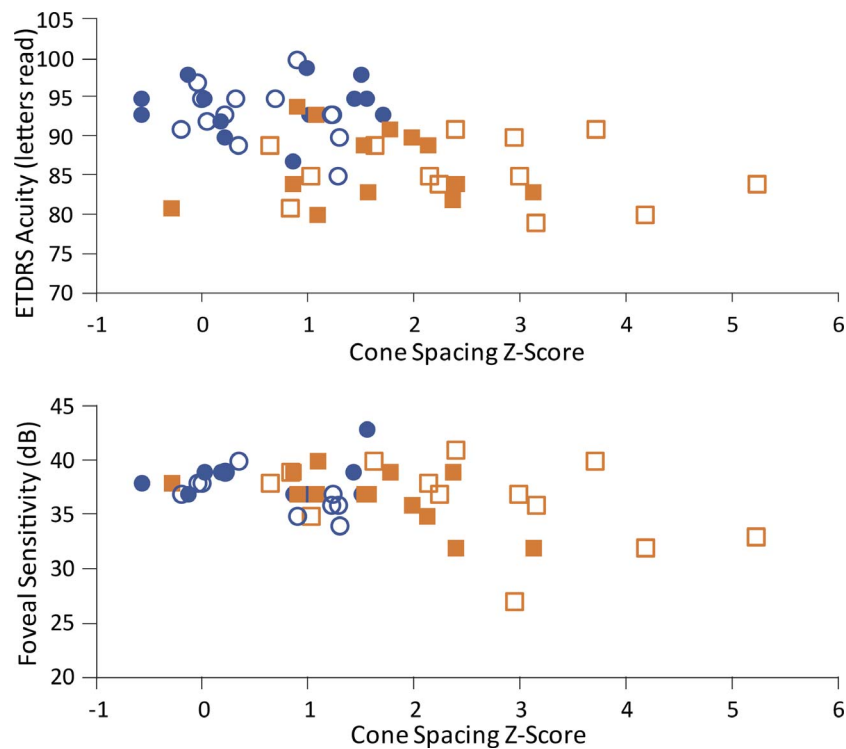


FIGURE 5. Visual acuity shown as ETDRS letters read (*top*) and foveal sensitivity (*bottom*) plotted against cone spacing Z-score. The cone spacing and visual acuity measures taken on the first imaging dates are in *filled symbols* and the second imaging dates are in *open symbols*; RCD patients are shown as *orange squares* and healthy subjects shown as *blue circles*. When all study subjects and visits were combined, cone spacing Z-score was significantly correlated with ETDRS letters read ($\rho = -0.47$, 95%CI -0.67 to -0.24) and foveal sensitivity ($\rho = -0.30$, 95%CI -0.52 to -0.018).

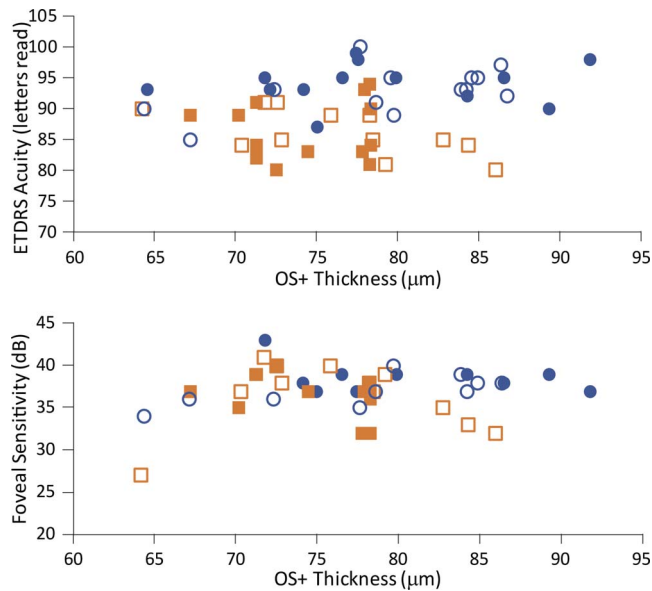


FIGURE 6. Outer segment plus retinal pigment epithelium and Bruch's membrane (OS+) thickness (μm) plotted against visual acuity shown as ETDRS letters read (*top*) and foveal sensitivity (dB) (*bottom*). The OS+ and visual acuity measures taken on the first imaging dates are in *filled symbols* and the second imaging dates are in *open symbols*; RCD patients are shown as *orange squares* and healthy subjects shown as *blue circles*. OS+ thickness was not significantly correlated with ETDRS letters read ($\rho = -0.11$, 95%CI -0.46 to 0.19) or foveal sensitivity when all subjects and visits were combined ($\rho = 0.026$, 95%CI -0.26 to 0.28).

The current study expanded our investigation with structural tests by also including OCT. A significant negative correlation between cone spacing Z-score and OS+ thickness at the PRL, where cone spacing increased as OS+ thickness decreased, was found in healthy subjects for both visits, but not at baseline or follow-up visit for RCD patients. The RCD patients in this study varied widely in the type and severity of their disease, which likely resulted in greater variability in the relationship between Z-score and OS+ thickness at the PRL. As seen in Figure 4, some patients retained well-preserved outer segments despite increased cone spacing Z-scores. Due to the proximity of the locations measured in the current study to the foveal center, we do not expect rod photoreceptors to have contributed to the OS+ thickness measures.

OS+ thickness was also compared with functional measures but was not significantly correlated with ETDRS letters read or with foveal sensitivity. In contrast, AOSLO-derived cone spacing Z-scores showed significant correlation with both visual acuity and foveal sensitivity.

The lack of a correlation might be real, or it could be that correlation is masked by noise from the measurement itself. While a full assessment of the noise of each measure is beyond the scope of this paper, some discussion of it is warranted. Regarding the functional measures, visual acuity measures are relatively robust (see later discussion on this point), but foveal sensitivity measurements reflect both intratest variability factors, such as neural background noise levels, and intervariability factors, such as reversible ocular and neural fluctuations.^{31,32} In addition, foveal sensitivity measures become more variable as visual function decreases. Therefore, RCD patients are more likely to have variable foveal sensitivity measures than the healthy subjects, which may explain why there was no correlation found between cone spacing Z-score and foveal sensitivity at follow-up. Regarding the AOSLO and SD-OCT structural measures, the

noise in both measures arises for different reasons. The SD-OCT system has a reported axial resolution of $7 \mu\text{m}$ and a pixel resolution of $3.5 \mu\text{m}$ ³³ and the OS+ measurement from the SD-OCT images used in this study comprised between 13 and 23 pixels. The use of a single trained grader (JLD) to manually segment a single horizontal B-scan centered on the PRL provides a further source of imprecision into the OS+ measures in the present study.^{5,6,22-24} AOSLO images have very fine lateral resolution of 0.58 arcmin ($\sim 2.5 \mu\text{m}$) and lateral sampling resolution of 0.14 arcmin/pixel ($\sim 0.7 \mu\text{m}/\text{pixel}$) but the distance between cones ranges from 3.5 to 7 pixels. These limits to cone spacing measurement are overcome in part by estimates of spacing from a collection of many intercone spacing measures.^{9,34} Despite the sources of noise and their impact, the final result was that structural cone measures from AOSLO proved to be more strongly correlated than SD-OCT with visual function in this study.

Limitations

The present study is limited in the number of eyes imaged with well-resolved cones visible near the fovea and is limited due to the retrospective nature with varied follow-up duration among the subjects. The inclusion of cone spacing measures as far from the PRL as 0.66° was not ideal but was necessary to ensure accurate visualization and measurement of cone spacing due to limited resolution of cones at the foveal center in some eyes. Given that fixation stability generally has a standard deviation of less than 0.1° ,³⁵ it is likely that in some subjects the cones in the retinal area we measured were never used for the acuity task. The conversion of cone spacing to Z-scores was done to overcome this limitation. Z-scores indicate the deviation in standard deviations from normal and are corrected for eccentricity. In this paper and in previous reports,^{9,11,36,37} we have noted greater than normal spacing and decreased densities throughout the central field of patients with RCD. The decreases in cone density may not be linear (i.e., density loss is greater toward the edges of the remaining visual field), but the degeneration appears to affect the entire retina, including the fovea, in the RCDs we have reported on to date.^{9,11,36-39} As such, we are confident that cone spacing Z-scores measured close to the fovea reflect cone spacing Z-scores at the fovea.

We chose to study foveal cones and compare with visual acuity even though the cone loss and degeneration—and consequent sensitivity to change—may be greater at the edges of degeneration. Not only did we do this because we were interested in foveal structure and function in these patients, but also because comparing structure and function outside of the fovea can be difficult. It has proven difficult to disambiguate cones and rods from other structures in confocal AOSLO images at the edge of degeneration in RCD patients.⁴⁰ Unfortunately, at the time that these images were collected phase-contrast imaging methods, like split-detector AOSLO⁴¹ were not available. In addition, whereas visual acuity represents a precise measure of visual function at the PRL and we made cone spacing measures as close as possible to the PRL, we did not have similar confidence that measures of visual function at the peripheral margins of degeneration would represent the function of the cones we quantified.

Finally, the fact that the healthy subjects in the current study were significantly older than the patients could underestimate the differences in cone spacing between healthy and patients, because cone density has been reported to be significantly lower in older, compared with younger, patients.⁴² Thus, our reports of increased cone spacing in the retinal degenerations patients may be considered conservative when compared with significantly older healthy subjects. However,

RCD is genetically heterogeneous and it is possible that in some forms of RCD there is nonuniform loss of cones; given the relatively small number of patients in the present study, we cannot compare cone patterns among patients with different genetic forms of retinal degeneration, but this would be an important question to study in future research.

Redundancy in Foveal Cones

Prior studies have suggested that the relationship between foveal structural measures and psychophysical measures is not linear.^{18,43} Using a theory that establishes resolvability as a measure directly proportional to the distance between foveal cones with intact connections to higher visual centers, 20/20 vision can be present with loss of 40% of foveal cones, 20/50 vision is expected with 10% of normal foveal cones, and 20/200 is expected with 1% of normal foveal cones.⁴³ Recent studies have used AOSLO to measure cone spacing near the fovea in eyes with retinal degeneration and have demonstrated that roughly 50% of cones can be lost before visual acuity declines below 20/25.^{17,18} Because clinical visual acuity can remain normal as foveal cone spacing increases, there is likely to be redundancy in foveal cones for high contrast and fine detail visual acuity tasks. The present results provide *in vivo*, longitudinal data to support predictions that cone density can decrease significantly before it manifests as a measurable decrease in visual acuity.

It is important to note that visual acuity is affected by more than just retinal sampling. Visual acuity integrates everything that occurs along the visual processing pathway, and each stage from where light first enters the eye to the generation of the visual percept can affect it. Moving from low- to high-order effects, the stages that govern visual acuity include (1) blur caused by imperfections in the eye's optics (low- and high-order aberrations),⁴⁴ (2) photoreceptor sampling, which is the focus of this study, (3) retinal ganglion cell receptive fields, which are generally considered to not impose a bottleneck for foveal vision in healthy eyes, but remodeling of the retinal in eye disease could change that,⁴⁵ (5) fixational eye movements, which have been shown to confer a benefit to foveal visual acuity,⁴⁶ and finally (6) all the post retinal, neural factors that can limit or interpret the sensory signals that come from the eye. These all need to be considered collectively to fully explain how acuity is preserved despite considerable cone loss.

Subtle Changes Need Finer Tools

Coupled with the redundancy in foveal cones to buffer the loss of visual impairment in eyes with RCD, the rate of decline in foveal vision in patients with retinal degeneration is slow.⁴⁷⁻⁴⁹ Moreover, factors such as the differences in patterns of visual field loss,^{50,51} genetic causes of RCD, and environment¹ may also contribute to variability in the rate of photoreceptor degeneration. Taken together, sensitive, objective measures of photoreceptor survival, such as cone spacing Z-scores from AOSLO images, may be more useful to monitor photoreceptor degeneration at the fovea than standard clinical measures, such as visual acuity, which are insensitive measures of disease progression in RCD. Foveal cone spacing measures may not be the most sensitive measurement of degeneration, especially in patients where cones are lost from the periphery inward; however, foveal cone degeneration will ultimately have the strongest effect on visual function and the patient's most precious cones. More sensitive tools may identify significant cone loss before changes in visual acuity and allow for earlier treatment to reduce disease progression as treatments become available. In a study that compared cone spacing in RCD

patients treated with sustained-release ciliary neurotrophic factor (CNTF) with sham-treated contralateral eyes, there was a significant increase in cone spacing and a reduction in cone density in the sham-treated RCD eyes, by 2.9% and 9.1%, respectively, over 24 to 36 months.¹¹ However, there was no significant change in visual acuity in either the CNTF- or sham-treated eyes.¹¹ Not only does this study reinforce the need for sensitive tools to diagnose and track disease progression of RCD but demonstrates the necessity for such tools in following up with treatments in RCD patients.

CONCLUSIONS

This study shows that cone spacing correlated with visual acuity in healthy subjects and RCD patients. However, as cone spacing increased in RCD patients over time, visual acuity did not concurrently change to reflect the progression of disease. Likewise, OS+ thickness did not change over time in RCD patients that demonstrated increased cone spacing, suggesting that cone spacing Z-score measured using adaptive optics ophthalmoscopy may be a more sensitive measure of cone loss at the fovea than measures of visual acuity or OS+ thickness in patients with RCD.

Acknowledgments

Supported by National Institutes of Health (NIH; Bethesda, MD, USA) Grant T32-EY007043 (EB), NIH Grants R01-EY023591, P30-EY003176, Foundation Fighting Blindness (AR, JD; Columbia, MD, USA), NIH Grant EY002162, FDA-OOPD grant R01-41001 (JD; Silver Spring, MD, USA), Research to Prevent Blindness (New York, NY, USA), The Claire Giannini Fund (JD; San Carlos, CA, USA), Hope for Vision (JD; Hollywood, FL, USA), The Bright Focus Foundation (JD; Clarksburg, MD, USA), The Bernard A. Newcomb Macular Degeneration Fund (JD; Mountain View, CA, USA), and That Man May See, Inc. (JD; San Francisco, CA, USA).

Disclosure: **E. Bensinger**, C. Light Technologies (C); **N. Rinella**, None; **A. Saud**, None; **P. Loumou**, None; **K. Ratnam**, None; **S. Griffin**, None; **J. Qin**, None; **T.C. Porco**, None; **A. Roorda**, P; **J.L. Duncan**, Neurotech USA Inc. (F), Allergan (F), Acucela (F), NightstarRx (F), Second Sight Medical Products (F), AGTC (S), ProQR Therapeutics (C, R, S), Spark Therapeutics (S), SparingVision (S), Editas Medicine Inc. (C), Ophthotech (C), Wave Life Sciences (C)

References

- Hartong DT, Berson EL, Dryja TP. Retinitis pigmentosa. *Lancet*. 2006;368:1795-1809.
- Holopigian K, Greenstein V, Seiple W, Carr RE. Rates of change differ among measures of visual function in patients with retinitis pigmentosa. *Ophthalmology*. 1996;103:398-405.
- Bittner AK, Ibrahim MA, Haythornthwaite JA, Diener-West M, Dagnelie G. Vision test variability in retinitis pigmentosa and psychosocial factors. *Optom Vis Sci*. 2011;88:1496-1506.
- Birch DG, Locke KG, Wen Y, Locke KI, Hoffman DR, Hood DC. Spectral-domain optical coherence tomography measures of outer segment layer progression in patients with X-linked retinitis pigmentosa. *JAMA Ophthalmol*. 2013;131:1143-1150.
- Hood DC, Lin CE, Lazow MA, Locke KG, Zhang X, Birch DG. Thickness of receptor and post-receptor retinal layers in patients with retinitis pigmentosa measured with frequency-domain optical coherence tomography. *Invest Ophthalmol Vis Sci*. 2009;50:2328-2336.
- Hood DC, Ramachandran R, Holopigian K, Lazow M, Birch DG, Greenstein VC. Method for deriving visual field bound-

- aries from OCT scans of patients with retinitis pigmentosa. *Biomed Opt Express*. 2011;2:1106-1114.
7. Smith TB, Parker M, Steinkamp PN, et al. Structure-function modeling of optical coherence tomography and standard automated perimetry in the retina of patients with autosomal dominant retinitis pigmentosa. *PLoS One*. 2016;11:e0148022.
 8. Hariri AH, Zhang HY, Ho A, et al. Quantification of ellipsoid zone changes in retinitis pigmentosa using en face spectral domain-optical coherence tomography. *JAMA Ophthalmol*. 2016;134:628-635.
 9. Duncan JL, Zhang Y, Gandhi J, et al. High-resolution imaging with adaptive optics in patients with inherited retinal degeneration. *Invest Ophthalmol Vis Sci*. 2007;48:3283-3291.
 10. Roorda A, Duncan JL. Adaptive optics ophthalmoscopy. *Annu Rev Vis Sci*. 2015;1:19-50.
 11. Talcott KE, Ratnam K, Sundquist SM, et al. Longitudinal study of cone photoreceptors during retinal degeneration and in response to ciliary neurotrophic factor treatment. *Invest Ophthalmol Vis Sci*. 2011;52:2219-2226.
 12. Merino D, Duncan JL, Tiruveedhula P, Roorda A. Observation of cone and rod photoreceptors in normal subjects and patients using a new generation adaptive optics scanning laser ophthalmoscope. *Biomed Opt Express*. 2011;2:2189-2201.
 13. Pircher M, Zawadzki RJ, Evans JW, Werner JS, Hitzenberger CK. Simultaneous imaging of human cone mosaic with adaptive optics enhanced scanning laser ophthalmoscopy and high-speed transversal scanning optical coherence tomography. *Opt Lett*. 2008;33:22-24.
 14. Rossi EA, Chung M, Dubra A, Hunter JJ, Merigan WH, Williams DR. Imaging retinal mosaics in the living eye. *Eye (Lond)*. 2011;25:301-308.
 15. Zhang T, Godara P, Blanco ER, et al. Variability in human cone topography assessed by adaptive optics scanning laser ophthalmoscopy. *Am J Ophthalmol*. 2015;160:290-300 e291.
 16. Wilk MA, Dubis AM, Cooper RF, Summerfelt P, Dubra A, Carroll J. Assessing the spatial relationship between fixation and foveal specializations. *Vision Res*. 2017;132:53-61.
 17. Foote KG, Loumou P, Griffin S, et al. Relationship between foveal cone structure and visual acuity measured with adaptive optics scanning laser ophthalmoscopy in retinal degeneration. *Invest Ophthalmol Vis Sci*. 2018;59:3385-3393.
 18. Ratnam K, Carroll J, Porco TC, Duncan JL, Roorda A. Relationship between foveal cone structure and clinical measures of visual function in patients with inherited retinal degenerations. *Invest Ophthalmol Vis Sci*. 2013;54:5836-5847.
 19. Curcio CA, Sloan KR, Kalina RE, Hendrickson AE. Human photoreceptor topography. *J Comp Neurol*. 1990;292:497-523.
 20. Zayit-Soudry S, Sippl-Swezey N, Porco TC, et al. Repeatability of cone spacing measures in eyes with inherited retinal degenerations. *Invest Ophthalmol Vis Sci*. 2015;56:6179-6189.
 21. Ferris FL III, Kassoff A, Bresnick GH, Bailey I. New visual acuity charts for clinical research. *Am J Ophthalmol*. 1982;94:91-96.
 22. Birch DG, Wen Y, Locke K, Hood DC. Rod sensitivity, cone sensitivity, and photoreceptor layer thickness in retinal degenerative diseases. *Invest Ophthalmol Vis Sci*. 2011;52:7141-7147.
 23. Wen Y, Klein M, Hood DC, Birch DG. Relationships among multifocal electroretinogram amplitude, visual field sensitivity, and SD-OCT receptor layer thicknesses in patients with retinitis pigmentosa. *Invest Ophthalmol Vis Sci*. 2012;53:833-840.
 24. Wen Y, Locke KG, Klein M, et al. Phenotypic characterization of 3 families with autosomal dominant retinitis pigmentosa due to mutations in KLHL7. *Arch Ophthalmol*. 2011;129:1475-1482.
 25. Cooper RF, Wilk MA, Tarima S, Carroll J. Evaluating descriptive metrics of the human cone mosaic. *Invest Ophthalmol Vis Sci*. 2016;57:2992-3001.
 26. Li KY, Tiruveedhula P, Roorda A. Intersubject variability of foveal cone photoreceptor density in relation to eye length. *Invest Ophthalmol Vis Sci*. 2010;51:6858-6867.
 27. Putnam NM, Hammer DX, Zhang Y, Merino D, Roorda A. Modeling the foveal cone mosaic imaged with adaptive optics scanning laser ophthalmoscopy. *Opt Express*. 2010;18:24902-24916.
 28. Wang Y, Bensaid N, Tiruveedhula P, Ma J, Ravikumar S, Roorda A. Human foveal cone photoreceptor topography and its dependence on eye length. *bioRxiv*. 2019;589135.
 29. Foote KG, De la Huerta I, Gustafson K, et al. Cone spacing correlates with retinal thickness and microperimetry in patients with inherited retinal degenerations. *Invest Ophthalmol Vis Sci*. 2019;60:1234-1243.
 30. Menghini M, Lujan BJ, Zayit-Soudry S, et al. Correlation of outer nuclear layer thickness with cone density values in patients with retinitis pigmentosa and healthy subjects. *Invest Ophthalmol Vis Sci*. 2014;56:372-381.
 31. Spry PG, Johnson CA. Identification of progressive glaucomatous visual field loss. *Surv Ophthalmol*. 2002;47:158-173.
 32. Owsley C, Jackson GR, Cideciyan AV, et al. Psychophysical evidence for rod vulnerability in age-related macular degeneration. *Invest Ophthalmol Vis Sci*. 2000;41:267-273.
 33. Heidelberg Engineering, GmbH. *Spectralis HRA+OCT Hardware Operating Instructions*. Heidelberg, Germany: Heidelberg Engineering; 2007.
 34. Rodieck RW. The density recovery profile: a method for the analysis of points in the plane applicable to retinal studies. *Vis Neurosci*. 1991;6:95-111.
 35. Barlow HB. Eye movements during fixation. *J Physiol*. 1952;116:290-306.
 36. Bowne SJ, Sullivan LS, Avery CE, et al. Mutations in the small nuclear riboprotein 200 kDa gene (SNRNP200) cause 1.6% of autosomal dominant retinitis pigmentosa. *Mol Vis*. 2013;19:2407-2417.
 37. Duncan JL, Biswas P, Kozak I, et al. Ocular phenotype of a family with FAM161A-associated retinal degeneration. *Ophthalmic Genet*. 2016;37:44-52.
 38. Duncan JL, Roorda A, Navani M, et al. Identification of a novel mutation in the CDHR1 gene in a family with recessive retinal degeneration. *Arch Ophthalmol*. 2012;130:1301-1308.
 39. Lew YJ, Rinella N, Qin J, et al. High-resolution imaging in male germ cell-associated kinase (MAK)-related retinal degeneration. *Am J Ophthalmol*. 2018;185:32-42.
 40. Sun LW, Johnson RD, Langlo CS, et al. Assessing photoreceptor structure in retinitis pigmentosa and Usher Syndrome. *Invest Ophthalmol Vis Sci*. 2016;57:2428-2442.
 41. Scoles D, Sulai YN, Langlo CS, et al. In vivo imaging of human cone photoreceptor inner segments. *Invest Ophthalmol Vis Sci*. 2014;55:4244-4251.
 42. Chui TY, Song H, Clark CA, Papay JA, Burns SA, Elsner AE. Cone photoreceptor packing density and the outer nuclear layer thickness in healthy subjects. *Invest Ophthalmol Vis Sci*. 2012;53:3545-3553.
 43. Geller AM, Sieving PA, Green DG. Effect on grating identification of sampling with degenerate arrays. *J Opt Soc Am A*. 1992;9:472-477.
 44. Rossi EA, Weiser P, Tarrant J, Roorda A. Visual performance in emmetropia and low myopia after correction of high-order aberrations. *J Vis*. 2007;7(8):14.
 45. Marc RE, Jones BW, Watt CB, Strettoi E. Neural remodeling in retinal degeneration. *Prog Retin Eye Res*. 2003;22:607-655.

46. Ratnam K, Domdei N, Harmening WM, Roorda A. Benefits of retinal image motion at the limits of spatial vision. *J Vis* 2017; 17(1):30.
47. Fishman GA, Bozbeyoglu S, Massof RW, Kimberling W. Natural course of visual field loss in patients with type 2 Usher syndrome. *Retina*. 2007;27:601-608.
48. Grover S, Fishman GA, Anderson RJ, Alexander KR, Derlacki DJ. Rate of visual field loss in retinitis pigmentosa. *Ophthalmology*. 1997;104:460-465.
49. Iannaccone A, Kritchevsky SB, Ciccarelli ML, et al. Kinetics of visual field loss in Usher syndrome type II. *Invest Ophthalmol Vis Sci*. 2004;45:784-792.
50. Grover S, Fishman GA, Gilbert LD, Anderson RJ. Reproducibility of visual acuity measurements in patients with retinitis pigmentosa. *Retina*. 1997;17:33-37.
51. Bittner AK, Iftikhar MH, Dagnelie G. Test-retest, within-visit variability of Goldmann visual fields in retinitis pigmentosa. *Invest Ophthalmol Vis Sci*. 2011;52:8042-8046.